Neural Representations of Temporally Modulated Signals in the Auditory Thalamus of Awake Primates

Edward L. Bartlett and Xiaoqin Wang

J Neurophysiol 97:1005-1017, 2007. First published Oct 18, 2006; doi:10.1152/jn.00593.2006

J Neurophysiol 97: 1005–1017, 2007.
First published October 18, 2006; doi:10.1152/jn.00593.2006.

Neural Representations of Temporally Modulated Signals in the Auditory Thalamus of Awake Primates

Edward L. Bartlett and Xiaoqin Wang

Laboratory of Auditory Neurophysiology, Department of Biomedical Engineering, Johns Hopkins University, Baltimore, Maryland

Submitted 5 June 2006; accepted in final form 17 October 2006

Bartlett EL, Wang X. Neural representations of temporally modulated signals in the auditory thalamus of awake primates. *J Neurophysiol* 97: 1005–1017, 2007. First published October 18, 2006; doi:10.1152/jn.00593.2006. In sensory systems, the thalamus has historically been considered a relay station. Neural representations of temporal modulations in the auditory system undergo considerable changes as they pass from the inferior colliculus (IC) to the auditory cortex. We sought to determine in awake primates the extent to which auditory thalamic neurons contribute to these transformations. We tested the temporal processing capabilities of medial geniculate body (MGB) neurons in awake marmoset monkeys using repetitive click stimuli. MGB neurons were able to synchronize to periodic clicks at repetition rates significantly higher than auditory cortex neurons. Unlike responses in the MGB of anesthetized animals, >40% of MGB neurons in awake marmosets displayed nonsynchronized discharges when stimulated by high click rates (short interclick intervals). Such nonsynchronized MGB responses typically occurred at higher repetition rates than those observed in auditory cortex. In contrast to auditory cortex neurons, many MGB neurons exhibited both synchronized and nonsynchronized discharge patterns. In both MGB and auditory cortex, synchronized and nonsynchronized responses represented complementary ranges of interclick intervals (1/click rate). Furthermore, the temporal processing abilities of some MGB neurons were sensitive to the spectrotemporal parameters of the click stimuli used. Together, these findings suggest that MGB neurons participate in active transformations of the neural representations of temporal modulations from IC to auditory cortex. In particular, the MGB appears to be the first station in the auditory ascending pathway in which substantial nonsynchronized responses emerge.

INTRODUCTION

The thalamus determines the nature of the incoming neural code to the cerebral cortex. A central question in sensory neuroscience is the extent to which the sensory thalamus is a "relay" of subthalamic sensory input (Sherman and Guillery 2002). Do thalamic neurons merely serve as state-dependent gates of sensory input or can they transform the neural representations that reach the cortex?

The way in which temporally modulated sound signals are encoded in the auditory thalamus serves as an interesting test case for investigating a coding transformation through the thalamus. Numerous studies of the inferior colliculus (IC), which is the auditory input to the thalamus, have shown that IC neurons represent time-varying sounds such as amplitude-modulated (AM) tones or noise by stimulus-synchronized discharges that are phase locked to the modulation envelope (Batra et al. 1989; Krishna and Semple 2000; Langner and Schreiner 1988; Muller-Preuss et al. 1994; for review see Joris et al. 2004), including one study of multiunit responses to AM stimuli in awake squirrel monkeys (Muller-Preuss et al. 1994). Although the firing rates of IC neurons also change in a modulation-frequency–dependent manner, the range of modulation frequencies over which IC neurons respond vigorously is typically the same range over which they are well synchronized with the stimulus (Joris et al. 2004; Krishna and Semple 2000). This is not the case in the auditory cortex of awake marmoset monkeys, where there are two main response types. Synchronized responses are phase locked to the stimulus, similar to reported IC responses (Liang et al. 2002; Lu et al. 2001a). Cortical synchronized responses occur mainly for low repetition rates (typically <50 Hz or 20-ms interclick intervals). The other main response type represents decreasing interclick intervals (increasing click rates) with monotonic increases in firing rate (Lu et al. 2001a). Thus temporal and rate representations are often dissociated in the auditory cortex but only rarely in the IC, although no studies have studied temporal processing in marmoset IC neurons. This transformation in response properties occurs either at the IC–medial geniculate body (MGB) synapse, the thalamocortical synapse, or intracortically. If nonsynchronized rate representations are prevalent in MGB neuronal responses, this would indicate that there is a conversion from a temporal to a rate code at the IC–MGB synapse.

Data from brain slice studies in the rat MGB have demonstrated two response patterns to repetitive electrical stimuli that are reminiscent of the synchronized and nonsynchronized responses observed in the auditory cortex (Bartlett and Smith 2002). One type produces large excitatory postsynaptic potentials (EPSPs) in MGB neurons and shows strong paired-pulse depression. At low stimulation frequencies, the synaptic responses produce highly entrained spiking in MGB neurons, similar to the synchronized responses observed in the auditory cortex in vivo. The other type produces small EPSPs and often shows paired-pulse facilitation. They generally respond poorly at low stimulation frequencies, instead requiring rapid stimulation frequencies for the EPSPs to summate and produce a suprathreshold response (Bartlett and Smith 2002), similar to the nonsynchronized responses in cortex. Thus the synaptic physiology of MGB neurons demonstrates that many MGB

Address for reprint requests and other correspondence: E. L. Bartlett or X. Wang, Johns Hopkins University, Dept. of Biomedical Engineering, Traylor 412, 720 Rutland Avenue, Baltimore, MD 21205 (E-mail: ebartle@purdue.edu or xiaoqin.wang@jhu.edu).

The costs of publication of this article were defrayed in part by the payment of page charges. The article must therefore be hereby marked "*advertisement*" in accordance with 18 U.S.C. Section 1734 solely to indicate this fact.

neurons are capable of producing nonsynchronized responses in vivo, at least in rodents.

Using repetitive click stimuli, we investigated the temporal processing capabilities of MGB neurons in the awake marmoset monkey. We found a significant alteration in MGB response properties compared with reported IC responses and compared with auditory cortex properties obtained from neurons recorded from the same preparation.

METHODS

Animal preparation and single-unit recording procedures

All experiments were performed at Johns Hopkins University in AAALAC approved facilities following protocols approved by the Institutional Animal Care and Use Committee (IACUC). The methods for preparing marmoset monkeys for electrophysiological recording and carrying out single-unit recordings in awake marmosets were previously reported (Bartlett and Wang 2005; Lu et al. 2001a,b). Some modifications were necessary for recording from MGB neurons and are described here.

The recording electrode approached the MGB in a dorsolateral to ventromedial trajectory. The electrode entered approximately 3 mm lateral to the lateral sulcus near its caudal end at an angle of 57.5°, where 0° is horizontal and 90° is vertical. The penetrations were at an angle 0° relative to the coronal plane (i.e., no change in rostrocaudal plane as the electrode was advanced). In animals whose auditory cortices had been mapped for different experiments, the insertion site for MGB was known to be lateral to the high-frequency representation of A1. Auditory-responsive neurons were encountered approximately 6–9 mm after penetrating the cortical surface (usually 6.5–7.0 mm). The rostral half of the MGB is bordered laterally by the lateral geniculate nucleus. Therefore it was possible to determine that the MGB was nearby when one passed through a region of visually responsive neurons followed by 200–700 μm without encountering any neurons.

The arousal state of the animal was monitored during experiments. Stimulus presentation and recording were halted or paused if the recording quality deteriorated or the animal was suspected to be drowsy when monitored through a camera placed inside the recording chamber (trials were resumed after the animal was confirmed to be awake with eyes open). Typically, one to three single units were fully studied in each recording session that lasted 3–5 h.

Acoustic stimuli

Stimuli were presented in free field from a speaker (B&W 601) located 70 cm in front of the animal and level with the animal's head (0° azimuth, 0° elevation). The interiors of the double-walled soundproof chambers (Industrial Acoustics) in which recordings took place were covered with 3-in. acoustic absorption foam (Sonex, Ilbruck, MN). Stimuli were created from custom programs using MATLAB software (The MathWorks, Natick, MA), generated through a D/A converter (Tucker-Davis Technologies, Alachua, FL) with a 100-kHz sampling rate, low-pass filtered at 50 kHz, attenuated with two serially linked attenuators (Tucker-Davis Technologies), and amplified by a power amplifier (Crown International, Elkhart, IN). The measured speaker output was within 4 dB of the intended output for frequencies from 100 Hz to 36 kHz, which encompasses the hearing range of marmosets, with a calibrated sound level of 90 dB SPL at 0 dB attenuation for 1-kHz tones.

The sound stimuli used were either 0.1-ms rectangular clicks or Gaussian clicks (Fig. 1, *A* and *B*). Gaussian clicks are tones, the amplitude envelope of which is a Gaussian function whose duration and bandwidth are determined by a variance parameter sigma (σ). Gaussian clicks were used to produce a spectral peak at the neuron's characteristic frequency (CF) and to avoid the activation of inhibitory sidebands. Examples of the individual click waveforms and power spectra are shown for 1-s train Gaussian clicks presented at 40-ms interclick intervals (25-Hz click rate). Each Gaussian click in this example had a carrier frequency of 5.0 kHz. Gaussian clicks were previously shown to be more effective than rectangular clicks at evoking responses in most auditory cortical neurons (Lu et al. 2001a). Gaussian clicks were set to the best frequency (BF) of the recorded neuron. Smaller sigma values produce shorter-duration clicks that have wider bandwidths, whereas the larger sigma values produce clicks with longer durations and narrower bandwidths (Fig. 1, *A* and *B*). To be consistent with the language of Lu et al. 2001a, temporal modulation will be discussed mostly in terms of interclick intervals (ICIs) rather than click rates (1/ICI).

MGB neurons were tested initially using rectangular clicks and with sigma parameters of 0.1, 0.2, and 0.4 at ICIs of 5, 40, and 75 ms

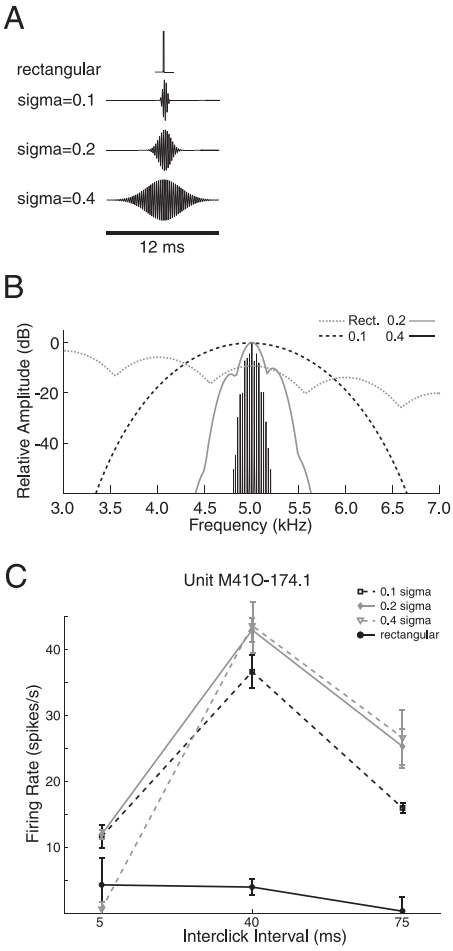

FIG. 1. Properties of the click stimuli and an example of click sigma preference. *A*: time–amplitude waveforms of individual click stimuli. Top stimulus is a 0.1-ms rectangular click. *Bottom 3 rows*: examples of the 3 Gaussian click stimuli used in this study, with a carrier frequency of 5.0 kHz in this example. Carrier frequency was matched to a unit's best frequency (BF) as determined by tone and noise responses. As click sigma increases, the Gaussian envelope becomes broader. *B*: Fourier spectra of 1-s, 25-Hz [40-ms interclick interval (ICI)] click trains using a 5.0-kHz carrier frequency for the Gaussian clicks. As click sigma increases, the power spectrum becomes narrower. *C*: example of the initial testing protocol used to identify click sigma preference, demonstrating lack of response to rectangular clicks. Rectangular clicks and Gaussian clicks of sigma = 0.1, 0.2, or 0.4 were used and tested at ICIs of 5, 40, and 75 ms, giving a basic profile of the click sigma preference of the neuron tested. For the unit shown (M41O-174.1), stimuli were delivered at 40-dB SPL. Firing rate was plotted as a function of ICI for each click sigma, demonstrating a clear preference for Gaussian clicks over rectangular clicks.

or 4, 10, 40, and 75 ms. Figure 1*C* illustrates the responses of an MGB neuron that responded only to Gaussian clicks (filled black and gray circles, open gray circles, 15.0-kHz carrier frequency) but not rectangular clicks (open black circles). For a given neuron, the smallest sigma that produced a sustained response or that produced a synchronized response was typically used to avoid the overlap of click waveforms. It was previously shown that IC neurons are sensitive to modulation depths of 20–30% (Krishna and Semple 2000). Using the variance parameter sigma as described above, a sigma of 0.4 produces a waveform with roughly 30% modulation depth for clicks presented at 5-ms ICI. Thus even for the largest sigma value used (sigma = 0.4), neurons in the IC that could project to MGB would be sensitive to envelope-modulation ICIs as low as 5 ms. The sound level of individual clicks was set at 0–10 dB above a neuron's best level, which was determined from tone or noise rate-level responses. For each neuron reported here, neurons were tested with click trains of 500- to 1,000-ms duration with a set of ICIs that varied from 1 to 100 or 1 to 150 ms. Spiking activity was recorded for 500 ms preceding each click train and for ≥500 ms after the offset of the sound stimulus. There was at least 1 s of silence between each stimulus. Each click train stimulus was repeated five to ten times.

Data analysis

MGB neurons ($n = 126$) from three animals were tested with click stimuli. Of those, 97 neurons produced significant responses, either as statistically significant increases in firing rate or as significant synchrony, and were analyzed further. Firing rate was computed for the entire stimulus duration. Spontaneous rate was computed as the mean rate of the 500-ms period that preceded each trial. The ability to synchronize to a click train was quantified by measuring the vector strength of the neuronal response at each ICI. Statistical significance was assessed using the Rayleigh statistic [$2 \times$ number of spikes $\times$ (vector strength)^2], which also takes into account the number of spikes evoked by the stimulus (Lu et al. 2001a; Mardia and Jupp 2000). For each ICI tested, the Rayleigh statistic was computed for the first half and second half of the stimulus and the minimum value was used. This excluded some responses that were synchronized during only part of the stimulus. A threshold Rayleigh statistic value of 13.8 was considered significant ($P < 0.001$).

For each unit, the minimum interclick interval at which the neuron significantly synchronized with the stimulus, called the synchronization boundary, was computed. This is the lower bound at which there will be significant synchronization to the click train. A linear interpolation was made between the Rayleigh value at the minimum ICI for which the unit was synchronized and the Rayleigh value for the next shorter ICI at which the unit was nonsynchronized (Lu et al. 2001a). The synchronization boundary was the ICI for which the Rayleigh value was 13.8. The maximum click rate at which the neuron was significantly synchronized was called Fmax, given by Fmax = 1/(synchronization boundary).

Many units produced nonsynchronized responses for short ICI stimuli. A rate boundary was computed for neurons that had statistically significantly driven firing rates (rank-sum test, $P < 0.05$ vs. spontaneous firing rate) in response to stimuli with ICI ≤5 ms. This is the upper boundary at which significant increases in firing rates are observed. A linear interpolation was made between the firing rate at the maximum ICI for which the unit was significantly driven and the firing rate for the next longer ICI at which the unit was not significantly driven (Lu et al. 2001a). The rate boundary was the ICI for which the interpolated driven firing rate crossed the threshold of twice the SD of the spontaneous rate.

Anatomy

At the cessation of recording, electrolytic lesions were made in physiologically identified regions of MGB by passing 2- to 10-μA current through the recording electrode (6–10 s each polarity). Animals were euthanized by administering an initial intramuscular injection of ketamine followed by an intraperitoneal injection of Euthasol (100 mg/kg; Virbac Australia).

Animals were transcardially perfused with room-temperature PBS with heparinized phosphate buffer (pH ≈ 7.0) followed by 4% paraformaldehyde (EM Grade, Ted Pella, Redding, CA) in 0.1 M phosphate buffer (pH ≈ 7.0). After perfusion, the brain was removed, put in 30% sucrose solution, and frozen. Sections (30 μm) were cut on a freezing microtome through the entire extent of the MGB. Sections were processed for Nissl staining, parvalbumin immunoreactivity, and calbindin immunoreactivity using standard histological procedures (Jones and Hendry 1989). Myelin staining used a modified Gallyas stain protocol (Pistorio et al. 2005).

MGB subdivisions were assigned based on parcellation schemes established in previous studies of the MGB in macaques (Hashikawa et al. 1995; Jones 2003; Kaas and Hackett 2000; Molinari et al. 1995), owl monkeys (Morel and Kaas 1992), and marmosets (Aitkin et al. 1988, 1993). The locations of recorded neurons in the MGB were reconstructed based on the coordinates of the tracks relative to the tracks in which lesions were made and the depths at which the recordings occurred. All analyzed units were recorded from the dorsal (anterodorsal and posterodorsal) and ventral divisions of the MGB (Jones 2003). A small number ($n = 6$) of units not included in the analysis were found in the medial division of MGB and the suprageniculate nucleus.

RESULTS

Of 126 MGB neurons, 97 (77%) tested with click stimuli had significant responses to one or more click stimuli. Of those, 87 neurons could be categorized into the three main response types described below, six neurons were not synchronized with the click stimuli and increased their firing rate with increasing ICI, and four neurons were inhibited by the click stimuli.

Response types

Response patterns to click stimuli typically fell into one of three main classes, shown in Fig. 2. Ninety-seven responses were analyzed from 87 units, with 10 units producing two different response types depending on the click sigma used (described later in detail). *Synchronized* (Synch) responses were observed in 16 units and consisted of discharges that were well entrained to the click train for long ICIs. At short ICIs, these neurons did not respond and were often inhibited after the onset response (14/16 units). The neuron in Fig. 2*A* produced highly synchronized discharges in response to rectangular click trains for ICIs from 10 to 150 ms, with the firing rate steadily decreasing from its peak at 10-ms ICI (100 Hz) as the ICI increased. This was a result of the decreased number of clicks in the stimulus with increasing ICI. Shorter ICIs from 4 to 7.5 ms resulted in a reduction of rate (Fig. 2*A*, solid line) and synchrony (Fig. 2*A*, dashed line) until the neuron produced an onset response only for 1- to 3-ms ICIs.

Nonsynchronized (Nonsynch) responses were observed in 41 neurons. These neurons did not have sustained synchrony in their responses for any of the ICIs tested. Eight of the 41 neurons classified as nonsynchronized exhibited synchrony in a portion of their response. Unlike synchronized or mixed responses, for which synchrony was evident over a wide range of interclick intervals (see Fig. 2, *A* and *C*), these eight neurons exhibited only limited, weak synchrony at one to two interclick intervals. The maximum vector strengths and mean vector

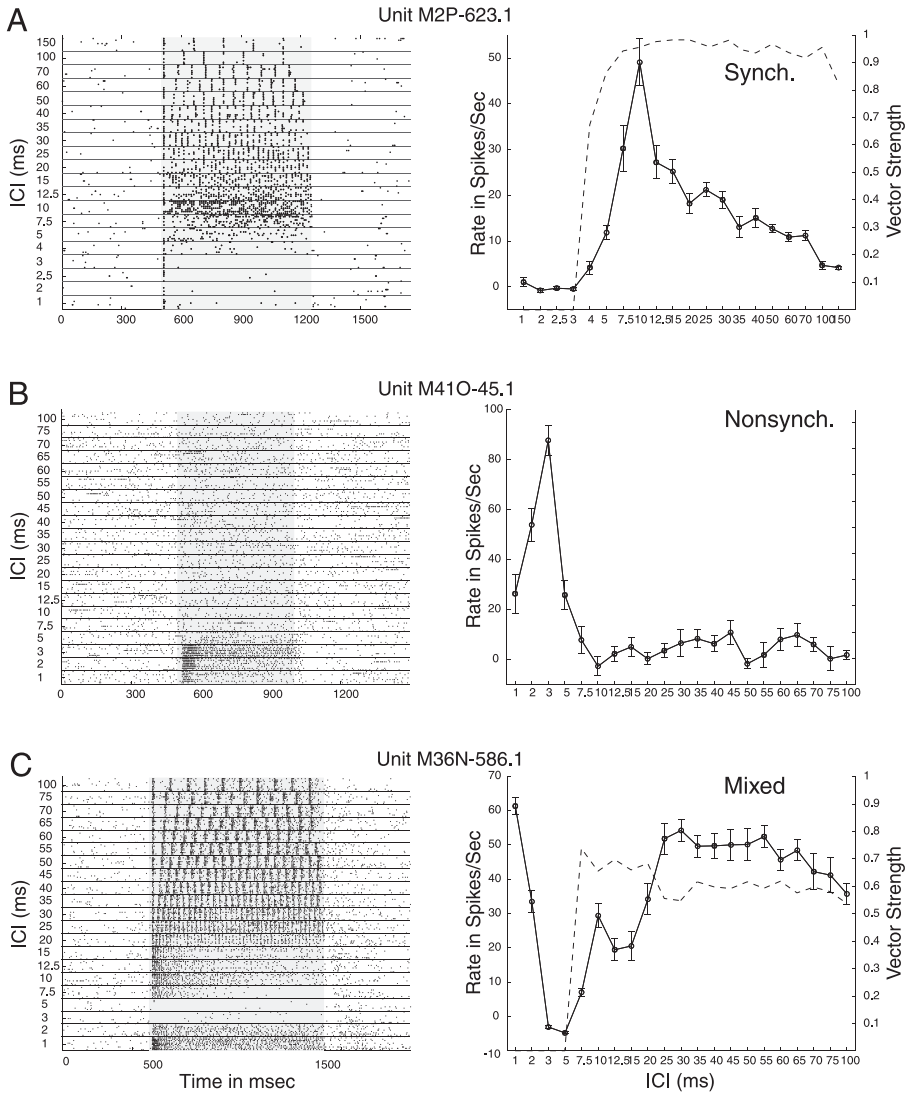

FIG. 2. Three main response types in medial geniculate body (MGB): synchronized, nonsynchronized, and mixed. *A*: unit M2P-623.1, sigma = rectangular click, characteristic frequency (CF) = 1.5 kHz (wideband onset), Level = 60 dB (all sound level dB values are dB SPL). *Left*: synchronized response dot raster (Synch response). Each dot represents one action potential. Shaded gray region shows the stimulus duration; white regions show the recorded pre- and poststimulus activity. *Right*: solid line plots firing rate as a function of ICI. Error bars are means ± SE. Dashed line plots vector strength as a function of ICI. Insignificant vector strengths in *A–C* have been set to zero. *B*: unit M41O-45.1, sigma = 0.1, CF = 6.96 kHz, Level = 30 dB. *Left*: nonsynchronized (Nonsynch) response dot raster. *Right*: firing rate vs. ICI. Same format as in *A*. No vector strengths were significant, so the right-hand axis was not displayed. *C*: unit M36N-586.1, sigma = 0.1, CF = 6.96 kHz, Level = 70 dB. *Left*: mixed (Mixed) response dot raster. *Right*: firing rate vs. ICI. Same format as in *A*. Note well-synchronized responses at long ICI and vigorous, nonsynchronized discharges for short ICI. Individual click waveforms were nonoverlapping at all ICIs tested in *A–C*.

strengths of these neurons were significantly smaller than those of either the synchronized or mixed populations (Kruskal–Wallis, $P < 0.001$). This shows that the weak, ICI-restricted synchrony exhibited by these neurons was quantitatively and qualitatively different from the synchrony exhibited by the other two response types.

Neurons with Nonsynch responses were typically not driven at long ICIs and mainly generated high discharge rates in response to ICIs ≤10 ms. The neuron in Fig. 2*B* was significantly driven only for ICI ≤5 ms. In this example, firing rate was nonmonotonic with respect to ICI and peaked for 3-ms ICI stimuli. This differs from what was observed in the nonsynchronized responses of auditory cortex neurons, whose rates almost always increased monotonically with decreasing ICI (Lu et al. 2001a). Of 41 neurons with Nonsynch responses, 14 were strongly nonmonotonic in their rate response, similar to the neuron in Fig. 2*B* (>50% change in firing rate between peak rate and rate in response to shortest ICI), 22/41 neurons were at least weakly nonmonotonic (>25% change in firing rate), and the firing rates of 17/41 neurons increased monotonically with decreasing ICI. Six nonsynchronized neurons were atypical in that they increased their firing rates with increasing ICI.

In contrast to purely synchronized or nonsynchronized responses, 40 neurons displayed responses that included two response regimes. These *Mixed* (Mixed) responses consisted of a stimulus-synchronized response at long ICIs and a nonsynchronized rate response at short ICIs. These response regimes were often separated by a range of ICIs over which the neuron was inhibited (20/40 units). In Fig. 2*C*, the neuron generated stimulus-synchronized responses and a vigorous firing rate for ICI from 7.5 to 100 ms. For ICIs from 3 to 5 ms, the neuron was clearly inhibited. Strong sustained firing occurred for ICIs from 1 to 2 ms. This response was nonsynchronized and the maximal firing rate exceeded that observed for longer ICIs when the response was synchronized. It should be noted that for the click sigma used for the stimulus (sigma = 0.1), the click waveforms were nonoverlapping. This meant that the depth of AM was 100%, even for a 1-ms ICI. The presence and prevalence of Mixed responses suggests that the intrinsic and synaptic mechanisms necessary to generate synchronized and nonsynchronized responses are present in single MGB neurons rather than forming separate neuronal populations.

Population averages of the firing rate, vector strength, and proportion of units synchronized are plotted in Fig. 3 for each response type as a function of ICI. Synch and Mixed responses

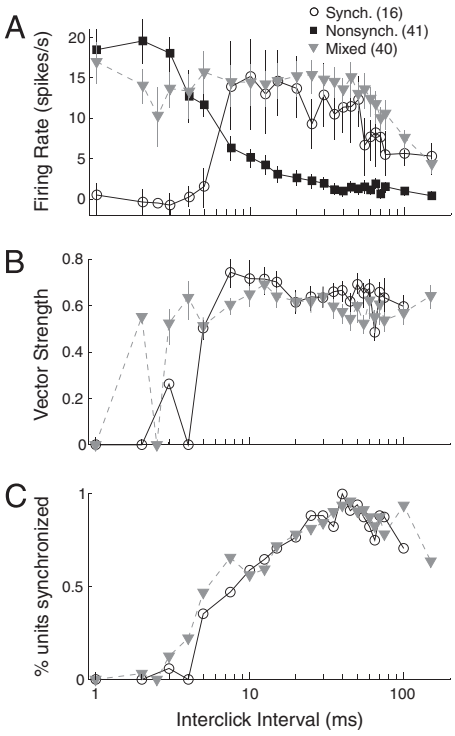

FIG. 3. Comparison of synchronized, nonsynchronized, and mixed MGB populations. *A–C*: open circles are for Synchronized responses (n = 16 responses), black squares are for Nonsynchronized (n = 41 responses), and gray triangles are for Mixed responses (n = 40 responses). *A*: firing rate vs. ICI for each response type. *B*: vector strength vs. ICI for each response type. *C*: proportion of units synchronized vs. ICI for each response type.

were on average driven at long ICIs, whereas Nonsynch responses were not (Fig. 3*A*). The average firing rates of Synch responses dropped dramatically for ICI <7.5 ms and were usually inhibited for ICI from 1 to 5 ms. In contrast, the firing rates of Mixed and Nonsynch responses were maximal or near maximal for short ICIs. In fact, Nonsynch firing rates did not begin to increase until ICIs were <50 ms and the Nonsynch rate response range was complementary to the Synch rate response range. Both Synch and Mixed firing rates were significantly higher than Nonsynch rates for all ICIs from 12.5 to 150 ms ($P < 0.05$, Kruskal–Wallis test), whereas Nonsynch and Mixed responses were significantly higher than Synch responses for 1- to 5-ms ICIs ($P < 0.05$, Kruskal–Wallis test). For the Synch and Mixed response populations, the vector strength of synchronized responses was consistently high for ICIs as low as 5 ms (Fig. 2*B*). The proportion of units that were stimulus synchronized (Fig. 2*C*) decreased with decreasing ICI and became very low for ICI <3 ms for both Synch and Mixed populations. Overall, 56 neurons produced stimulus-synchronized discharges. Almost half (26/56 = 46%) of the Synch and Mixed neurons were still phase locked at 5-ms ICI, but only (9/56 = 17%) were still phase locked at 3-ms ICI, suggesting that this was approaching the upper bound for phase locking in the MGB. Only two units were phase locked at 2-ms ICI.

Responses types were also separable by comparing the distributions of the ICIs that generated the maximum and minimum firing rates (Fig. 4*A*). Synchronized responses were typically maximal at ICIs >10 ms and minimal at ICIs ≤5 ms (Fig. 4*A*, open circles). By contrast, nonsynchronized firing rates were typically maximal at ICIs ≤5 ms and minimal at ICIs >10 ms (Fig. 4*A*, black squares). Depending on whether the maximum firing rate occurred in the synchronized or nonsynchronized portions of the Mixed response, the ICIs were widely distributed (Fig. 4*A*, gray triangles).

On average, Mixed responses generated the highest maximum firing rates (Fig. 4*B*) and were significantly higher than Nonsynch responses ($P < 0.005$, Kruskal–Wallis) but not Synch responses. Approximately half of the Mixed neurons generated their highest firing rates for ICIs that were lower than their synchronization boundary (21/40 = 52%). This meant that the highest firing rates in these neurons were in the nonsynchronized portion of their response.

The nonsynchronized responses of auditory cortex neurons generally increased monotonically with decreasing ICI (Lu et al. 2001a). By contrast, the responses of 34% (14/41) of Nonsynch responses and 50% (20/40) of Mixed responses exhibited a clear preference for ICI, such that responses to 1-ms ICI click trains were ≥50% lower than the maximum response (Fig. 4*B*).

There was no significant difference in the temporal precision of Synch or Mixed responses as assessed by the mean vector strength averaged over all ICIs (Fig. 4*C*) or the maximum vector strength (Kruskal–Wallis, $P > 0.05$). There was also no significant difference between the ICIs that produced the highest value of the Rayleigh statistic value, which is a measure of the maximal sustained synchronized response (Kruskal–Wallis, $P > 0.05$). Only 14/56 (25%) responses produced the maximum Rayleigh for ICIs ≥100 Hz, with most neurons in the 20- to 80-Hz range.

The different types of responses were not associated with systematic differences in the BFs of the neurons. Moreover, the nonsynchronized responses were not attributable to responses to click rates at or near BF in almost all cases. Figure 4*D* plots the normalized distribution of BFs derived from tone or noise responses for neurons with synchronized responses (combined Synch and Mixed populations, open white bars) and nonsynchronized responses (black bars). Synchronized and nonsynchronized responses were found in units over a wide range of BFs and there was no significant difference between the two BF distributions (Kruskal–Wallis, $P > 0.05$). The BFs of the vast majority of units were well outside of the range at which any of the click rates used would impinge on the unit's frequency receptive field (synchronized units 25–75% of distribution = 2.1–11.3 kHz, nonsynchronized units 25–75% of distribution = 3.2–10.5 kHz). Only 11 units had BFs <1.5 kHz and only five units had BFs <1.0 kHz.

Although the type of response evoked was not dependent on sigma, there was a difference in the synchronization boundaries between the largest sigma used (0.4) and the other sigmas used (rectangular, 0.1, 0.2). Figure 4*E* shows the distribution of click sigmas that generated Synch (n = 16, open bars), Nonsynch (n = 41, black bars), and Mixed (n = 40, gray bars) responses. Each type of response was observed at all sigmas, although there was a slight tendency for synchronized responses to be produced by larger click sigmas (8/16 synchronized responses were produced by click sigma = 0.4). Figure 4*F* plots the distributions of the synchronization boundaries at each sigma. There were no significant differences between the synchronization boundaries for units tested with rectangular clicks, sigma = 0.1, or sigma = 0.2 (Kruskal–Wallis, $P >$

0.05). However, all three groups had lower synchronization boundaries than those of units tested with sigma = 0.4 clicks (Kruskal–Wallis, $P < 0.05$). This makes sense because for sigma = 0.4, individual clicks fused and the click train envelope was basically flat for ICI <5 ms. Note that if a unit was tested with two sigmas, the sigma associated with the shortest synchronization boundary was used.

Comparison of MGB and cortical responses

For each MGB neuron, the synchronization boundary and the rate boundary were computed (see METHODS). If a unit was tested with two or more different click sigmas or sound levels, the response that had the shortest synchronization boundary was chosen for analysis. Figure 5*A* shows the distribution of

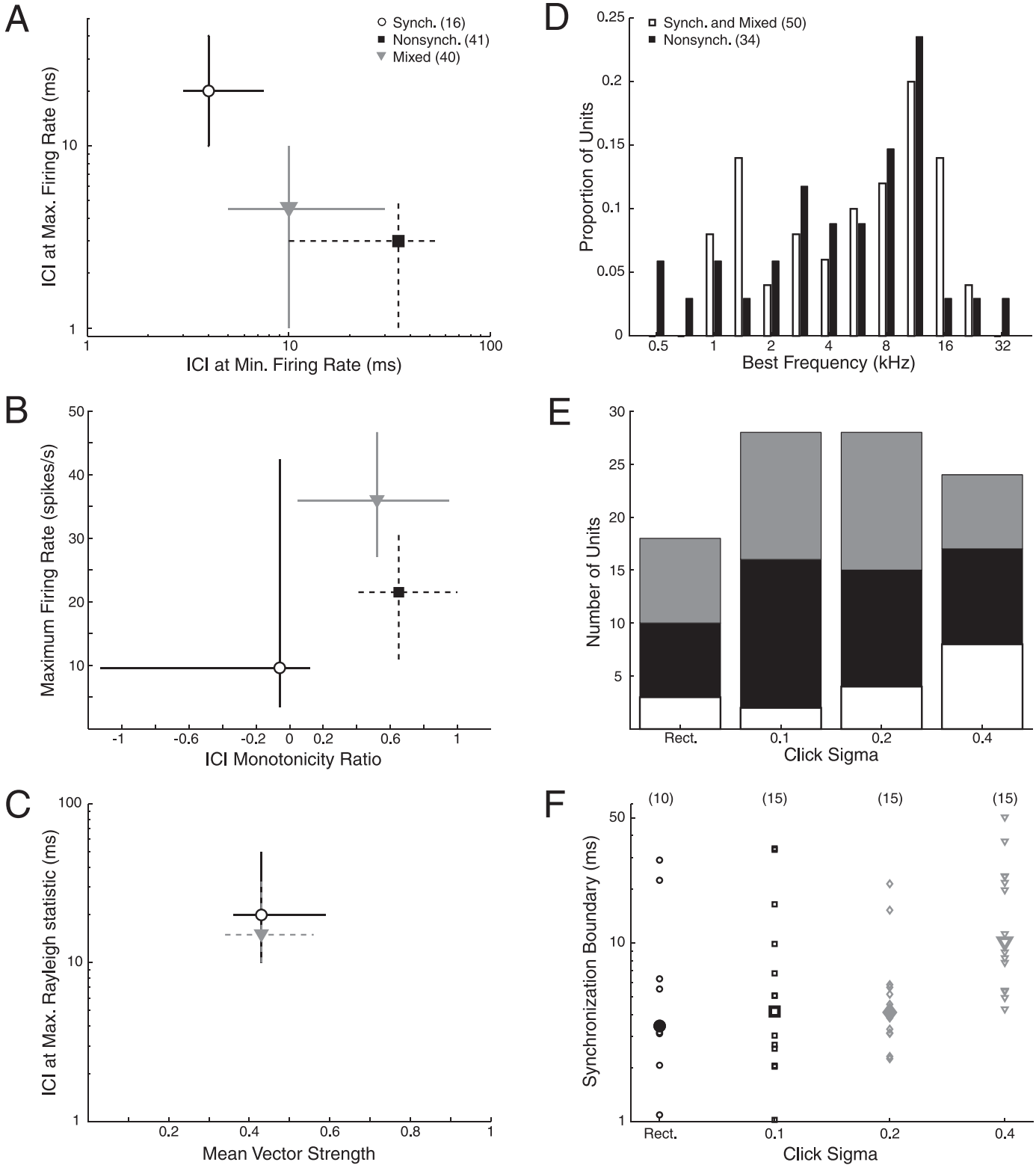

synchronization boundaries for the Synch and Mixed response types compared with the synchronization boundaries of auditory cortex neurons in awake marmosets from Lu et al. (2001a). MGB neurons had much shorter synchronization boundaries than those of auditory cortex neurons. Most commonly the MGB synchronization boundary was between 4 and 7 ms (median = 5.2 ms, 25–75% = 3.3–11.4 ms, $n = 56$ neurons). This was approximately 2 octaves higher in terms of frequency than the median value for auditory cortex neurons in awake marmosets (Fig. 5*A*, solid line, median = 21.3 ms, 25–75% = 12.4–54.3 ms; Lu et al. 2001a). MGB Synch responses tended to have higher synchronization boundaries than Mixed responses, with 14/16 Synch responses having boundaries ≥5-ms ICI, compared with 18/40 Mixed responses (Fig. 5*A*, *inset*, $P < 0.01$, χ^2 test).

Just as the synchronization boundaries were shifted to shorter ICIs, the rate boundaries of MGB neurons were also shifted to shorter ICIs compared with cortical neurons (Fig. 5*B*). The distributions of rate boundaries were similar for Nonsynch and Mixed responses, suggesting that they arose as the result of similar mechanisms. The median rate boundary of MGB neurons was 5.7 ms (25–75% = 4.0–10.0 ms) (Fig. 5*B*), compared with a median rate boundary of 12.9 ms (25–75% = 9.9–21.3 ms) in marmoset auditory cortex (Lu et al. 2001a). Interestingly, the values in the auditory cortex of the pentobarbital-anesthetized cat (Lu and Wang 2000; median = 6.3 ms, 25–75% = 5.2–9.7 ms), for which the relative contribution of thalamocortical afferents would be enhanced as the result of a general suppression of cortical activity, were very similar to the values in the marmoset MGB. The synchronized and nonsynchronized populations of neurons in the MGB and cortex represented complementary ICI ranges by phase-locked temporal representations and nonsynchronized rate representation. Figure 5*C* compares the complementarity of MGB and cortex populations by looking at vector strength as a measure of phase locking (gray lines) and normalized firing rate as a measure of rate representation (black lines). At short ICIs ≤3 ms, the MGB firing rate of nonsynchronized neurons was near maximal. Then it decreased rapidly from 3 to 10 ms. Over this same ICI range, the MGB population vector strength of the combined Synch and Mixed populations increased rapidly. By 10-ms ICI, the MGB representations have clearly segregated (Fig. 5*C*), whereas the cortex representations are not clearly segregated until 20- to 30-ms ICIs.

One question that we had was whether the nonsynchronized responses were initiated and generated by the auditory cortex. If this were the case, we would expect that the latency of the cortical nonsynchronized responses would be shorter than the MGB latencies. For each unit, the latency of the response was calculated. On average, the latencies of Synch and Mixed responses were significantly shorter than synchronized responses in the auditory cortex (Kruskal–Wallis test, $P = 0.02$) (Fig. 6*A*). The median MGB synchronized response latency was 15.5 ms ($n = 46$), whereas the median cortex latency was 20.5 ms ($n = 36$). Nonsynchronized responses in MGB and auditory cortex occurred at much longer latencies than synchronized responses in both MGB and auditory cortex neurons (Fig. 6*B*). The median MGB nonsynchronized response latency was 49.8 ms ($n = 39$) and the distribution of MGB nonsynchronized response latencies overlapped extensively with auditory cortex latencies (median = 46.0 ms, $n = 50$). Therefore we cannot determine from these data whether nonsynchronized responses are initiated by MGB or auditory cortex neurons.

Neurons with Mixed responses generated synchronized responses at long ICIs and nonsynchronized responses at short ICIs. This allowed us to compare the latencies of the synchronized portions and nonsynchronized portions of the responses in individual neurons and to compare the latencies of the nonsynchronized portions of Mixed responses with those of Nonsynch responses. We examined the latencies of the synchronized and nonsynchronized responses separately in 22 neurons with Mixed responses for which latencies could be determined for both responses. The latencies of the synchronized responses (median = 15.6 ms) were shorter than the latencies of the nonsynchronized responses (median = 29.3 ms) in 20/22 Mixed neurons (Fig. 6*C*, $P < 0.001$, signed-rank sum). However, the latencies of the nonsynchronized portions of Mixed responses (median = 30.4 ms) were significantly shorter than those with purely nonsynchronized responses (median = 49.8 ms) (Kruskal–Wallis, $P < 0.02$), suggesting that the latencies of Mixed neurons at short ICI may be influenced by additional excitatory inputs compared with Nonsynch neurons.

Shifts in response pattern arising from changes in click width

A critical issue in temporal processing by single units is whether the observed temporal processing properties are invariant with respect to the carrier. In other words, are neurons more sensitive to the periodicity of the temporal envelope, regardless of the details of the modulation waveform such as spectrum, duration, and envelope shape? To investigate this issue, we tested 38 neurons with two or more different click sigma over the full range of ICIs. Note that this differs from our initial testing for click sigma preference, described in METHODS, for which we sampled only three to four different ICIs. As shown in Fig. 1, altering the click sigma from

FIG. 4. Further comparison of synchronized, nonsynchronized, and mixed MGB populations. *A*: ICI that produced the maximum firing rate was plotted as a function of the ICI that produced the minimum firing rate for Synch (open circles), Nonsynch (black squares), and Mixed (gray triangles) responses. Large symbols show the median values for each population in *A–C* and lines show the 25–75% values along each dimension. Legend in *A* applies to *A–C* and *E*. *B*: plot of maximum firing rate as a function of the ICI Monotonicity Ratio for the 3 response types. ICI Monotonicity Ratio = (Maximum Firing Rate)/(Firing Rate for 1 ms ICI). *C*: ICI that produced the maximum value of the Rayleigh statistic [2 × number of spikes × (vector strength)^2] was plotted as a function of the mean vector strength averaged over all ICIs. Because this formulation of the Rayleigh is an approximation for large numbers of spikes, it is worth noting that the Rayleigh statistic for the vast majority of units (85/97 units) was computed using ≥40 spikes and 77% of the units (75/97) using ≥80 spikes. Thus the approximation for large numbers of spikes was almost always appropriate. There were no significant differences between the Mixed and Synch responses. *D*: histogram comparing the BFs of neurons with synchronized responses (combined Synch and Mixed, $n = 50$) with BFs of neurons with only nonsynchronized responses ($n = 34$). There were no significant differences between the 2 groups (Kruskal–Wallis, $P > 0.05$). BFs were obtained from tone or noise frequency receptive fields. *E*: histogram showing the distribution of click sigmas that produced each click response type. Open bars are for Synch responses, black bars are for Nonsynch responses, and gray bars are for Mixed responses. *F*: distributions of synchronization boundaries were plotted as a function of the click sigma that was used. Numbers in parentheses indicate number of units for each sigma. For a given unit, the sigma that was associated with the shortest synchronization boundary was used.

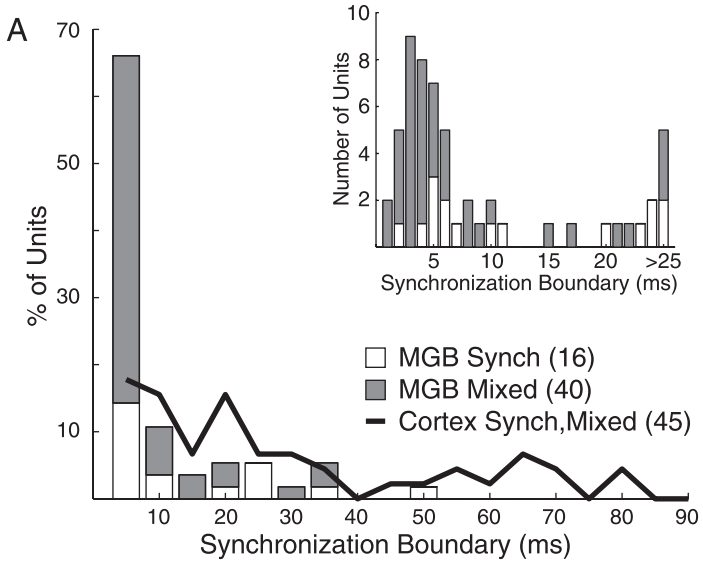

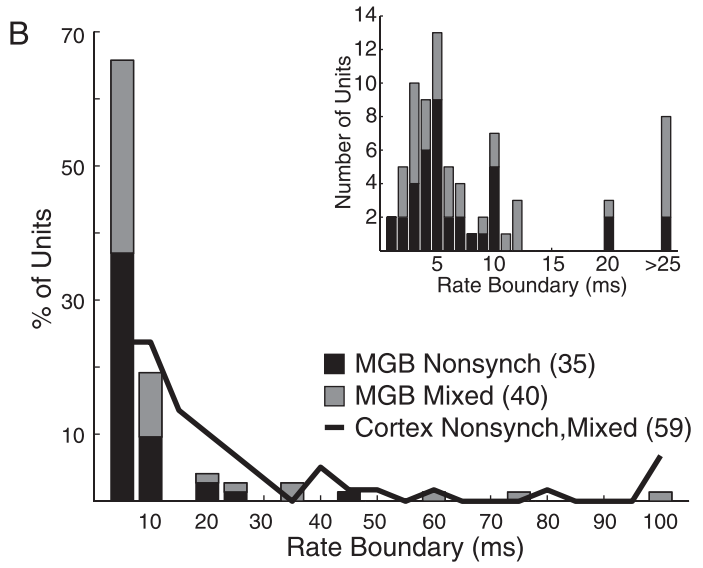

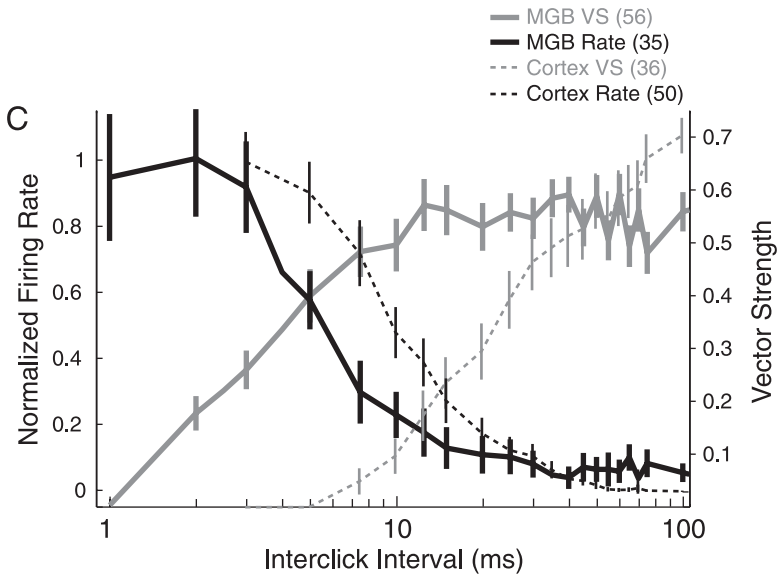

FIG. 5. MGB synchronization and rate boundaries are shifted to lower ICIs compared with auditory cortex. *A*: normalized histogram of the minimum ICI at which neurons can synchronize (synchronization boundary). Open bars are Synchronized responses; gray bars are Mixed responses. Solid black line plots the histogram of synchronization boundaries in auditory cortex neurons from Lu et al. (2001a). *A*, *inset*: MGB synchronization boundaries are replotted in 1-ms bins. Same legend as in *A*. *B*: histogram of the rate boundaries (see METHODS). Black bars are Nonsynchronized responses; gray bars are Mixed responses. The solid black line plots the histogram of rate boundaries in auditory cortex neurons from Lu et al. (2001a). *B*, *inset*: MGB rate boundaries are replotted in 1-ms bins. Same legend as in *B*. *C*: mean ± SE of vector strength of MGB Synchronized and Mixed responses (thick gray solid lines) and normalized firing rate of MGB Nonsynchronized responses (thick black solid lines) as a function of ICI. Mean ± SE of vector strength of auditory cortex Synchronized responses (thin gray dashed lines) and normalized firing rate of auditory cortex Nonsynchronized responses (thin black dashed lines) as a function of ICI. Cortex data are from Lu et al. (2001a).

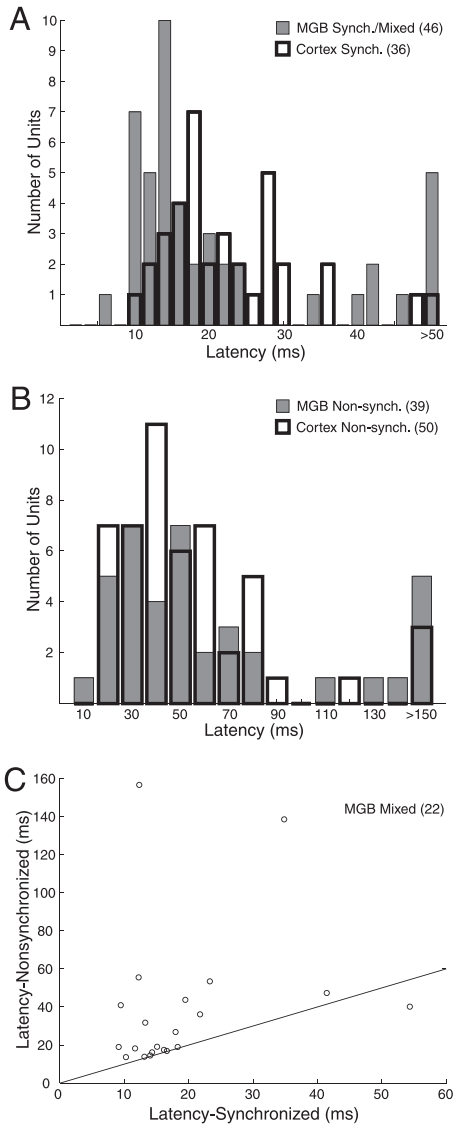

FIG. 6. Nonsynchronized MGB and cortical latencies are not significantly different, but synchronized MGB and cortical latencies are. *A*: histogram of latencies of synchronized and mixed MGB responses (gray bars) and of synchronized auditory cortex responses (open thick lined bars). *B*: histogram of latencies of nonsynchronized MGB responses (gray bars) and of nonsynchronized auditory cortex responses (open thick lined bars). Cortex latency data were obtained from the data used in Lu et al. (2001a). *C*: latencies of the synchronized (x-axis) and nonsynchronized portions (y-axis) of the MGB response were calculated for 22 neurons that produced significant firing rates in both regimes. Line indicates $x = y$, and 20/22 neurons had longer latencies for the nonsynchronized response ($P < 0.001$, paired rank sum).

rectangular to 0.1 up to 0.4 substantially decreases the bandwidth of the click stimulus while simultaneously increasing the duration of individual clicks and increasing the duration of each individual click (see Fig. 1).

A few neurons exhibited dramatic differences in their response patterns when the click sigma changed. An extremely striking example of these differences is shown in Fig. 7, *A* and *B*. This example was used to illustrate high sensitivity to click sigma, but such high sensitivity was observed in only a small minority of cases. Responses in Fig. 7, *A* and *B* were evoked by Gaussian click trains with the same CF and sound level and covering the same ICI range. The only difference was that $\sigma =$ 0.4 in Fig. 7*A* and $\sigma = 0.1$ in Fig. 7*B*. When $\sigma = 0.4$, the neuron was well synchronized for all stimuli with ICIs from 15 to 100 ms and it fired only weakly in response to shorter ICI stimuli (Fig. 7*A*). When $\sigma = 0.1$, the neuron did not respond at all until the ICI was 10 ms. Even then, it fired vigorously for ICIs only from 3 to 7.5 ms (Fig. 7*B*), so this response pattern was complementary to the response pattern observed when $\sigma = 0.4$. This can be seen clearly in Fig. 7*C*. The long ICIs that produced sustained firing and well-synchronized responses in Fig. 7*A* did not drive the unit at all in Fig. 7*B*. Note also that even when the firing rates were similar for 7.5-ms ICI stimuli, the latency of the response was much longer in Fig. 7*B* than in Fig. 7*A*.

Of the 38 neurons tested with more than one click sigma, 11 neurons produced nonsynchronized responses for all sigma values tested. For these 11 neurons, the click rates that produced the maximum firing rates shifted by less than one octave in four of 11 neurons. Of 11 neurons with only nonsynchronized responses seven changed their preferred click rate by more than one octave.

Twenty-seven neurons produced synchronized responses for at least one sigma. For each of these neurons, the synchronization boundaries were computed for the smallest and largest click sigma values tested. Of 27 neurons only nine changed their Fmax (1/synchronization boundary) by less than one octave. Together, the temporal coding of 13/38 (9 synchronized + 4 nonsynchronized = 34%) neurons was therefore insensitive to the click stimuli used. However, 18/27 of units changed their Fmax by more than one octave. Thus 25/38 neurons (18 synchronized + 7 nonsynchronized = 66%) were sensitive to the spectrotemporal parameters of the click stimuli and 10/38 (26%) neurons changed their representation of modulation rate from synchronized to nonsynchronized when click sigma changed.

Despite this sensitivity to the click stimuli in some neurons, the sensitivity was predictable. We compared the synchronization boundaries for the 27 neurons that were synchronized for at least one click sigma. If a neuron generated synchronized responses for short-duration, spectrally broad clicks (rectangular clicks or sigma = 0.1), then it would usually also produce synchronized responses for long-duration, spectrally narrow clicks (sigma = 0.2 or 0.4). However, the converse was not true. The neurons that were most sensitive to click sigma generally synchronized only to sigma = 0.2 or 0.4 because these clicks were long enough in duration to evoke a response.

These observations are shown graphically in Fig. 7*D*. When the shorter synchronization boundary was observed for the smallest click sigma (Fig. 7*D*, open circles below $y = x$ line, $n = 14$), the synchronization boundary was generally very short and did not change much when the click sigma changed. When the shorter synchronization boundary was observed for the largest click sigma (Fig. 7*D*, gray triangles above $y = x$ line, $n = 13$), the synchronization boundary was generally longer and was quite sensitive to the click sigma. In fact, seven of ten neurons that were synchronized at one sigma and nonsynchronized at another click sigma were synchronized only for the largest click sigma. Neurons whose boundaries were shorter for the smallest sigma (Fig. 7*D*, open circles) had significantly shorter boundaries at the smallest and largest sigma values than neurons whose shorter boundaries were for

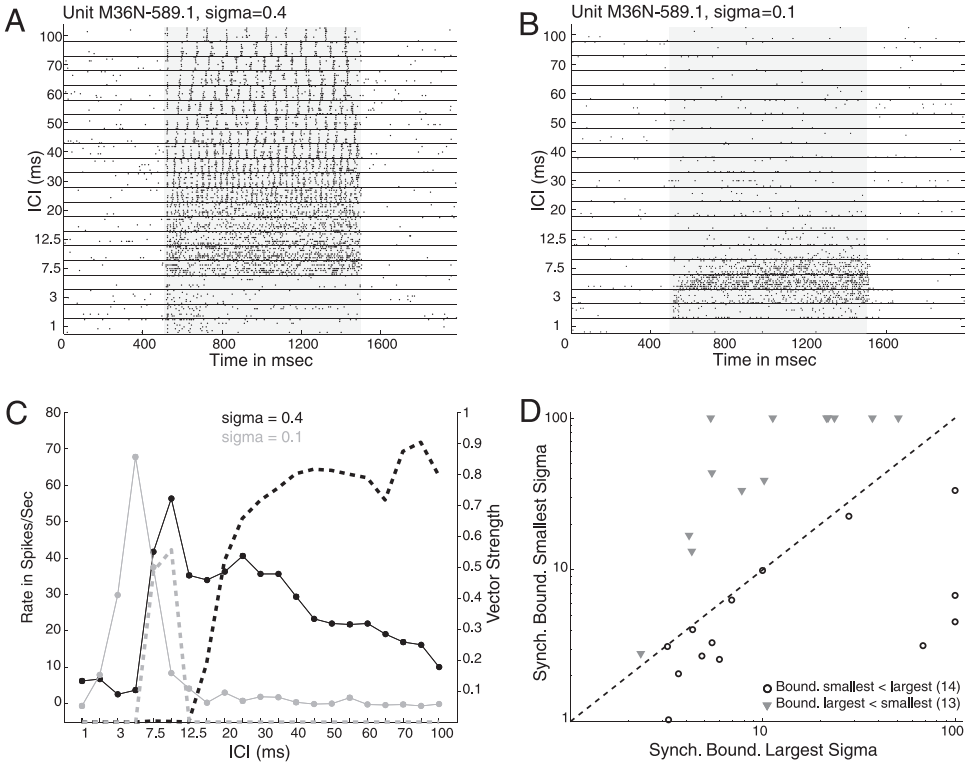

FIG. 7. Responses of some MGB neurons are sensitive to shifts in click sigma. *A*: unit 1–589.1, CF = 10.85 kHz, $\sigma = 0.4$, Level = 30 dB. Narrow-band, long-duration click stimulus generated short-latency, well-synchronized responses for ICIs 15–100 ms. *B*: changing sigma to 0.1 resulted in a click with a wider bandwidth and a shorter-duration click. This resulted in no response for long ICI stimuli and long-latency responses for 3- to 7.5-ms ICI stimuli. *C*: plot of firing rate (solid lines) and vector strength (dashed lines) for the rasters in *A* and *B*. Values for $\sigma = 0.4$ are plotted in black; values for $\sigma = 0.1$ are plotted in gray. *D*: 27 neurons were tested with at least 2 different click sigmas and produced synchronized responses for at least one sigma. For each neuron, the synchronization boundaries were computed for the smallest and largest click sigmas tested over the full ICI range. Synchronization boundary for the smallest sigma was plotted vs. the synchronization boundary for the largest sigma. Synchronization boundaries of nonsynchronized responses were set to 100-ms ICI, the longest ICI typically tested. Dashed line is the $y = x$ line. Open circles represent neurons whose synchronization boundary was shorter for the smallest sigma; gray triangles represent neurons whose synchronization boundary was shorter for the largest sigma.

the largest sigma values (Fig. 7*D*, gray triangles, $P < 0.05$, Kruskal–Wallis). Furthermore, neurons whose boundaries were shorter for the smallest sigma (Fig. 7*D*, open circles) had significantly smaller differences between synchronization boundaries tested at different sigmas (i.e., closer to the $y = x$ line, $P < 0.05$, Kruskal–Wallis). These results suggest that some MGB neurons are highly sensitive to the spectrotemporal parameters of the overall stimulus, not just the ICI. Those neurons that synchronize poorly or not at all to short-duration, spectrally broad clicks appear to be particularly sensitive to parameters other than ICI. Conversely, some neurons appear able to phase lock at short ICI regardless of the click stimulus parameters, particularly those that synchronize well to short-duration clicks. These neurons may be specialized for rapid temporal processing.

DISCUSSION

Summary of results

We have demonstrated that MGB responses to temporally modulated stimuli differ from reported IC and auditory cortex responses to repetitive auditory stimuli. This implies that the MGB does not act as a simple relay and that there are sequential transformations of temporal coding from IC to MGB to cortex. Unlike reported IC responses, both stimulus-synchronized temporal and nonsynchronized rate representations were observed in MGB responses to repetitive click trains. Many individual MGB neurons were able to encode low click rates with a temporal representation and high click rates with a rate representation. With the appearance of nonsynchronized firing rate responses to encode high click rates, the MGB is the first auditory nucleus for which there is a complete dissociation of high synchrony and high firing rate. Some MGB neurons dramatically changed their discharge patterns when the click width changed, implying that the temporal processing capabilities of some MGB neurons depend on stimulus parameters other than the temporal modulation rate.

Comparison with previous studies of inferior colliculus

The representations of temporally modulated (sAM) stimuli were previously investigated extensively in the cat (Escabi and Schreiner 2002; Langner and Schreiner 1988), rat (Rees and Møller 1983,1987), bat (Burger and Pollak 1998; Condon et al. 1994), gerbil (Krishna and Semple 2000), rabbit (Batra et al. 1989), and squirrel monkey (Muller-Preuss et al. 1994). Of these studies, only Batra et al. (1989; single-unit) and Muller-Preuss et al. (1994; multiunit) recorded in unanesthetized animals. IC neurons typically have band-pass or weakly modulated rate responses and band-pass or low-pass synchrony responses. Responsive IC neurons were always synchronized for some range of modulation frequencies, with synchronization boundaries in the range of 2–16 ms (Joris et al. 2004). Thus the distribution of MGB synchronization boundaries in the present study is similar to what has been reported in IC (see Fig. 5*A*). The main difference between reported IC responses and the MGB responses in our study appears to be in the abundance of MGB neurons that did not respond significantly to low click rates and responded to high click rates only with nonsynchronized discharges. However, it is possible that some IC neurons are not phase locked to the stimulus and participate in the generation of nonsynchronized MGB responses (Escabi and Schreiner 2002; Muller-Preuss et al. 1994). Another possibility is that the abundance of nonsynchronized responses reflects a specialization found in primates but not in other species, although this remains to be tested.

Comparison with previous studies of MGB

Previous studies investigating the temporal processing abilities of MGB neurons observed primarily phase-locked responses (Creutzfeldt et al. 1980; Miller et al. 2002; Preuss and Muller-Preuss 1990; Rouiller and deRibaupierre 1982; Rouiller et al. 1981; Vernier and Galambos 1957), although neurons sometimes produced onset responses for high click rates. Our observation that the median Fmax of MGB neurons (192 Hz) is significantly higher than auditory cortex (47 Hz) confirms at the population level what was suggested by examples recorded from the awake guinea pig (Creutzfeldt et al. 1980).

However, none of the previous studies reported the large number of nonsynchronized responses that we have observed. In some cases (Miller et al. 2002; Rouiller et al. 1981), this may have been the result of anesthetics that reduced sustained excitation produced by activation of *N*-methyl-D-aspartate (NMDA) receptors (Krystal et al. 2003; Villars et al. 2004). In studies using unanesthetized animals, either the range of repetition rates tested was below the range of most nonsynchronized responses (Preuss and Muller-Preuss 1990) or the emphasis of the study was on synchronized responses (Creutzfeldt et al. 1980; Vernier and Galambos 1957).

It should be noted that one multiunit study in awake macaques found responses to clicks at very high rates (≤800 Hz) in the putative thalamorecipient lamina in auditory cortex (Steinschneider et al. 1998). However, these responses occurred at sites whose BFs were matched to the preferred click rates, which differs from the nonsynchronized responses that we have reported. For the most part, the click rates that evoked nonsynchronized responses in our study were well outside of the frequency receptive field of the neurons (Fig. 4*D*). Only 11/70 neurons that produced nonsynchronized responses had BFs ≤1.5 kHz. Of those, only six of 11 had 50% response bandwidths that would produce a response to frequencies <1 kHz, which was the highest click rate tested.

The prevalent nonsynchronized responses that we observed did not arise from a fusion of click waveforms. Over 80% of nonsynchronized responses (34/41 nonsynchronized responses) produced significant rate responses at ICIs corresponding to distinct click waveforms and all of the other neurons produced significant responses at ICIs for which there was some fusion but still clear AM of the sound envelope (>30% modulation depth). It is possible that the use of Gaussian clicks biased the responses toward nonsynchronized responses because of their spectral peak and limited bandwidth relative to rectangular clicks. However, rectangular clicks also produced nonsynchronized responses in 13 neurons.

Comparison with previous studies of auditory cortex

Although MGB neurons exhibited synchronized and nonsynchronized responses, they differed from the synchronized and nonsynchronized responses observed in auditory cortex neurons using the same experimental preparation (awake marmoset) (Lu et al. 2001a). The ICI ranges covered by the synchronized and nonsynchronized discharges were shifted to shorter ICIs (Fig. 5*C*). The rate boundaries of MGB neurons were also shifted to shorter ICIs (Fig. 5*C*). Nonsynchronized responses from the auditory cortex of anesthetized cats had rate boundaries similar to those reported here (Lu and Wang 2000), suggesting that the nonsynchronized responses observed in the anesthetized auditory cortex reflected the responses of the thalamocortical inputs. More important than the simple shifts toward shorter ICI in the MGB was the prevalence of Mixed responses in the MGB compared with the IC or auditory cortex. This suggests that the MGB is beginning the transition between the synchronized and nonsynchronized responses that becomes more distinct in cortex.

Sensitivity to spectrotemporal parameters

Approximately two thirds (25/38) of the neurons tested with more than one click sigma exhibited a significant shift in their response, shifting either their Fmax or their preferred click rate by more than one octave (Fig. 7). Thus the temporal processing abilities of most neurons were stimulus dependent. Only one third of the MGB neurons were insensitive to the spectrotemporal stimulus parameters with respect to temporal processing. Neurons whose responses were stimulus dependent typically generated better synchronized responses for larger-click sigma values and poorly synchronized or nonsynchronized responses for smaller click sigma values (Fig. 7). For these neurons, this implies that despite the shorter duration and therefore increased temporal localization of the smaller sigma stimuli (Fig. 1*A*), synchronization was generally better in response to the longer-duration envelopes with sharper spectral peaks.

One possibility is that differences in the energy at or near the neuron's best frequency might be responsible for the stimulus dependency. However, similar to auditory cortex neurons (Lu et al. 2001a), energy normalization did not change the temporal response properties of MGB neurons ($n = 6$ MGB neurons tested). Moreover, despite large changes in the bandwidths of stimuli with different sigma values, it seems unlikely that the sensitivity to click sigma was attributable to shifting the click spectrum into or out of the neuron's pure-tone frequency receptive field. Of the 38 neurons tested with more than one sigma, seven of 38 had BFs <1.5 kHz. None of these neurons switched from Nonsynch to Synch. All of the neurons whose behavior changed from Nonsynch to Synch had BFs 6–20 kHz, so the Nonsynch activity was almost definitely not the result of direct excitation (see Fig. 1*B* for example with 5.0-kHz carrier).

Another possibility is that the neurons require a minimum stimulus duration to produce sustained synchronization, making it more likely that better synchronization will occur for the larger-click sigma values. We conclude that many MGB neurons will respond to a repetitive stimulus if there is energy at their best frequency, but the exact nature of the response will depend not only on the stimulus repetition rate, but also on the carrier spectrum and envelope duration in a predictable manner. Similar sensitivity to the carrier's fine structure and envelope shape was also previously observed in IC (Rees and Møller 1987) and auditory cortex (Lu et al. 2001b).

Potential mechanisms for generating synchronized and nonsynchronized responses

MGB synchronized discharges originate from the synchronized inputs of IC neurons, but the Fmax of many MGB neurons is lower than that of IC neurons. Inhibition apparently

regulates the maximum repetition rate at which many MGB neurons can synchronize (Fig. 2, *A* and *C*). Inhibition could arise from local MGB interneurons (Sherman 2004) or from the feedforward inhibitory projection from the IC (Peruzzi et al. 1997), which can strongly affect the magnitude and timing MGB postsynaptic potentials (Bartlett and Smith 1999, 2002), similar to the way in which inhibition influences spike generation in auditory cortex (Wehr and Zador 2003).

Another inclusive possibility is that two classes of IC excitatory inputs to MGB neurons determine the response pattern. Data from rat brain slices demonstrated that one type of IC excitatory input generates large, short-latency inputs that exhibit strong paired-pulse depression (Bartlett and Smith 2002). These inputs would reliably propagate IC synchronized discharge patterns at low repetition rates, but the sustained synchronized response would eventually disappear at high repetition rates, similar to what was observed in Synch and Mixed responses (Fig. 3). The other type of IC excitatory input generates smaller, longer-latency inputs that exhibit paired-pulse facilitation at short interstimulus intervals (Bartlett and Smith 2002). Neurons receiving these inputs would be unlikely to respond to long ICI stimuli because multiple small inputs would be required to reach firing threshold. Instead, they would respond to short ICI stimuli when the small inputs could summate to generate a longer-latency suprathreshold response, which is supported by the differences in the latencies of synchronized and nonsynchronized responses (Fig. 6). Activation of NMDA receptors in these neurons would produce sustained excitation that would bolster weak responses and smear temporal precision, both of which were previously observed in MGB and auditory cortex neurons in vitro (Bartlett and Smith 2002; Rose and Metherate 2005). This could result in nonsynchronized responses in MGB neurons.

MGB is not merely a relay station

The MGB is not a simple relay of IC inputs. The main difference between IC and cortex representations of repetition rate appears to be in the creation of separate synchronized and nonsynchronized responses. Then the MGB acts as a transition stage in this transformation, with the emergence of nonsynchronized responses and the prevalence of mixed responses. A transition stage from IC to MGB to cortex was recently observed for the integration of tone and noise responses (Las et al. 2005). Figure 8 depicts the transformation of temporal representations suggested by our study by comparing the response types across regions using data from three studies that recorded from single units in awake animals. The IC study looked at single-unit responses in awake rabbits (Batra et al. 1989) and the MGB and cortex studies were done using awake marmosets (Lu et al. 2001a; present study). As a population, MGB neurons may create separate temporal and rate coding populations that could potentially represent temporal and spectral features, respectively. Complementary MGB rate and synchronization boundaries (Fig. 5*C*) are near perceptual boundaries of periodicity perception versus perception of fine structure, a transition from spectrotemporal to purely spectral features (Rosen 1992). Rate responses at short ICIs in the absence of synchronized responses at longer ICIs is a response pattern that first appears in the MGB and is quite prevalent. Such a transformation of response pattern indicates that MGB neurons are not simple relays and contribute to the neural representations of sound features that serve as the inputs to auditory cortex.

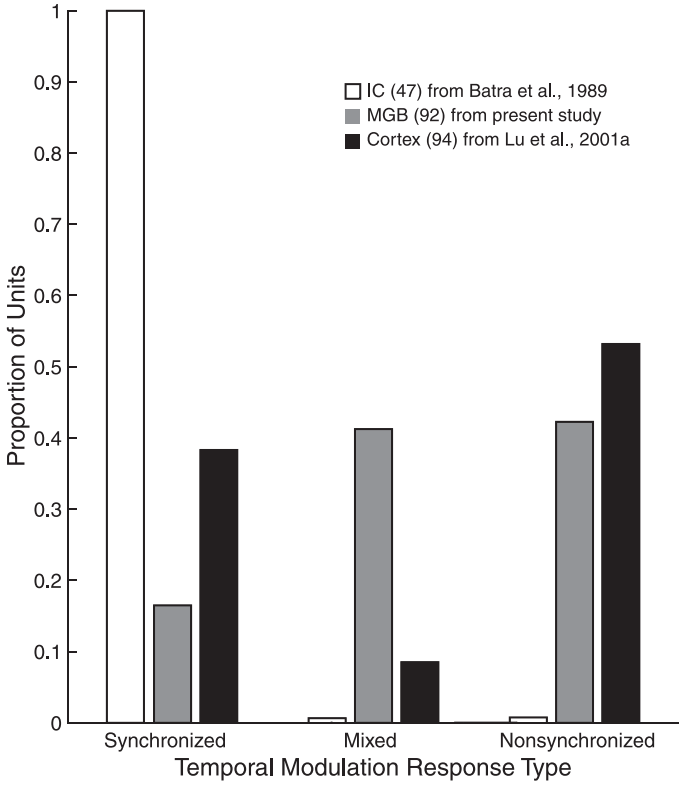

FIG. 8. MGB transitions the transformation from a synchronized representation in IC to synchronized and nonsynchronized representations in auditory cortex. Proportion of units in each auditory region (IC, MGB, Auditory Cortex) is plotted for each representation of temporal modulation (Synchronized, Mixed, Nonsynchronized). IC data are from Batra et al. (1989). Auditory cortex data are from Lu et al. (2001a). Total number of units from each region is shown in parentheses.

ACKNOWLEDGMENTS

We thank A. Pistorio for excellent assistance in animal maintenance and neuroanatomy; S. Hendry for generous use of facilities, materials, and expertise; and D. Bendor and E. Issa for helpful comments on a draft of the manuscript.

Present address of E. L. Bartlett: Purdue University, Depts. of Biological Sciences and Biomedical Engineering, 206 S. Intramural Drive, BMED 2023, West Lafayette, IN 47907-1791.

GRANTS

This work was supported by Deafness Research Foundation Grant BAE.HOPK-03-1C and National Institute on Deafness and Other Communication Disorders Grants DC-06357 to E. Bartlett and DC-03180 to X. Wang.

REFERENCES

Aitkin L, Park V. Audition and the auditory pathway of a vocal New World primate, the common marmoset. *Prog Neurobiol* 41: 345–367, 1993.

Aitkin LM, Kudo M, Irvine DR. Connections of the primary auditory cortex in the common marmoset, *Callithrix jacchus jacchus*. *J Comp Neurol* 269: 235–248, 1988.

Bartlett EL, Smith PH. Anatomic, intrinsic, and synaptic properties of dorsal and ventral division neurons in rat medial geniculate body. *J Neurophysiol* 81: 1999–2016, 1999.

Bartlett EL, Smith PH. Effects of paired-pulse and repetitive stimulation on neurons in the rat medial geniculate body. *Neuroscience* 113: 957–974, 2002.

Bartlett EL, Wang X. Long-lasting modulation by stimulus context in primate auditory cortex. *J Neurophysiol* 94: 83–104, 2005.

Batra R, Kuwada S, Stanford TR. Temporal coding of envelopes and their interaural delays in the inferior colliculus of the unanesthetized rabbit. *J Neurophysiol* 61: 257–268, 1989.

Burger RM, Pollak GD. Analysis of the role of inhibition in shaping responses to sinusoidally amplitude-modulated signals in the inferior colliculus. *J Neurophysiol* 80: 1686–1701, 1998.

Calford MB. The parcellation of the medial geniculate body of the cat defined by the auditory response properties of single units. *J Neurosci* 3: 2350–2364, 1983.

Condon CJ, White KR, Feng AS. Processing of amplitude-modulated signals that mimic echoes from fluttering targets in the inferior colliculus of the little brown bat, *Myotis lucifugus. J Neurophysiol* 71: 768–784, 1994.

Creutzfeldt O, Hellweg FC, Schreiner C. Thalamocortical transformation of responses to complex auditory stimuli. *Exp Brain Res* 39: 87–104, 1980.

Escabi MA, Schreiner CE. Nonlinear spectrotemporal sound analysis by neurons in the auditory midbrain. *J Neurosci* 22: 4114–4131, 2002.

Hashikawa T, Molinari M, Rausell E, Jones EG. Patchy and laminar terminations of medial geniculate axons in monkey auditory cortex. *J Comp Neurol* 362: 195–208, 1995.

Hu B. Functional organization of lemniscal and nonlemniscal auditory thalamus. *Exp Brain Res* 153: 543–549, 2003.

Hu B, Senatorov V, Mooney D. Lemniscal and non-lemniscal synaptic transmission in rat auditory thalamus. *J Physiol* 479: 217–231, 1994.

Jones EG. Chemically defined parallel pathways in the monkey auditory system. *Ann NY Acad Sci* 999: 218–233, 2003.

Jones EG, Hendry SHC. Differential calcium binding protein immunoreactivity distinguishes classes of relay neurons in monkey thalamic nuclei. *Eur J Neurosci* 1: 222–246, 1989.

Joris PX, Schreiner CE, Rees A. Neural processing of amplitude-modulated sounds. *Physiol Rev* 84: 541–577, 2004.

Kaas JH, Hackett TA. Subdivisions of auditory cortex and processing streams in primates. *Proc Natl Acad Sci USA* 97: 11793–11799, 2000.

Krishna BS, Semple MN. Auditory temporal processing: responses to sinusoidally amplitude-modulated tones in the inferior colliculus. *J Neurophysiol* 84: 255–273, 2000.

Krystal JH, D'Souza DC, Mathalon D, Perry E, Belger A, Hoffman R. NMDA receptor antagonist effects, cortical glutamatergic function, and schizophrenia: toward a paradigm shift in medication development. *Psychopharmacology (Berl)* 169: 215–233, 2003.

Langner G, Schreiner CE. Periodicity coding in the inferior colliculus of the cat. I. Neuronal mechanisms. *J Neurophysiol* 60: 1799–1822, 1988.

Las L, Stern EA, Nelken I. Representation of tone in fluctuating maskers in the ascending auditory system. *J Neurosci* 25: 1503–1513, 2005.

Liang L, Lu T, Wang X. Neural representations of sinusoidal amplitude and frequency modulations in the primary auditory cortex of awake primates. *J Neurophysiol* 87: 2237–2261, 2002.

Lu T, Liang L, Wang X. Temporal and rate representations of time-varying signals in the auditory cortex of awake primates. *Nat Neurosci* 4: 1131–1138, 2001a.

Lu T, Liang L, Wang X. Neural representations of temporally asymmetric stimuli in the auditory cortex of awake primates. *J Neurophysiol* 85: 2364–2380, 2001b.

Lu T, Wang X. Temporal discharge patterns evoked by rapid sequences of wide- and narrowband clicks in the primary auditory cortex of cat. *J Neurophysiol* 84: 236–246, 2000.

Mardia KV, Jupp PE. *Directional Statistics.* New York: Wiley, 2000.

Miller LM, Escabi MA, Read HL, Schreiner CE. Spectrotemporal receptive fields in the lemniscal auditory thalamus and cortex. *J Neurophysiol* 87: 516–527, 2002.

Molinari M, Dell'Anna ME, Rausell E, Leggio MG, Hashikawa T, Jones EG. Auditory thalamocortical pathways defined in monkeys by calcium-binding protein immunoreactivity. *J Comp Neurol* 362: 171–194, 1995.

Morel A, Garraghty PE, Kaas JH. Tonotopic organization, architectonic fields, and connections of auditory cortex in macaque monkeys. *J Comp Neurol* 335: 437–459, 1993.

Morel A, Kaas JH. Subdivisions and connections of auditory cortex in owl monkeys. *J Comp Neurol* 318: 27–63, 1992.

Muller-Preuss P, Flachskamm C, Bieser A. Neural encoding of amplitude modulation within the auditory midbrain of squirrel monkeys. *Hear Res* 80: 197–208, 1994.

Peruzzi D, Bartlett E, Smith PH, Oliver DL. A monosynaptic GABAergic input from the inferior colliculus to the medial geniculate body in rat. *J Neurosci* 17: 3766–3777, 1997.

Pistorio AL, Hendry SH, Wang X. A modified technique for high-resolution staining of myelin. *J Neurosci Methods* 153: 135–146, 2006.

Preuss A, Muller-Preuss P. Processing of amplitude modulated sounds in the medial geniculate body of squirrel monkeys. *Exp Brain Res* 79: 207–211, 1990.

Rees A, Møller AR. Responses of neurons in the inferior colliculus of the rat to AM and FM tones. *Hear Res* 10: 301–330, 1983.

Rees A, Møller AR. Stimulus properties influencing the responses of inferior colliculus neurons to amplitude-modulated sounds. *Hear Res* 27: 129–143, 1987.

Rosen S. Temporal information in speech: acoustic, auditory and linguistic aspects. *Philos Trans R Soc Lond B Biol Sci* 336: 367–373, 1992.

Rouiller E, de Ribaupierre F. Neurons sensitive to narrow ranges of repetitive acoustic transients in the medial geniculate body of the cat. *Exp Brain Res* 48: 323–326, 1982.

Rouiller E, de Ribaupierre Y, Toros-Morel A, de Ribaupierre F. Neural coding of repetitive clicks in the medial geniculate body of cat. *Hear Res* 5: 81–100, 1981.

Schreiner CE, Sutter ML. Topography of excitatory bandwidth in cat primary auditory cortex: single-neuron versus multiple-neuron recordings. *J Neurophysiol* 68: 1487–1502, 1992.

Sherman SM, Guillery RW. The role of the thalamus in the flow of information to the cortex. *Philos Trans R Soc Lond B Biol Sci* 357: 1695–1708, 2002.

Vernier VG, Galambos R. Response of single medial geniculate units to repetitive click stimuli. *Am J Physiol* 188: 233–237, 1957.

Villars PS, Kanusky JT, Dougherty TB. Stunning the neural nexus: mechanisms of general anesthesia. *AANA J* 72: 197–205, 2004.

Wenstrup JJ. Frequency organization and responses to complex sounds in the medial geniculate body of the mustached bat. *J Neurophysiol* 82: 2528–2544, 1999.

Winer JA. The functional architecture of the medial geniculate body and primary auditory cortex. In: *The Mammalian Auditory Pathway: Neuroanatomy*, edited by Fay RR, Popper AN, Webster DB. New York: Springer-Verlag, 1992, p. 222–409.